DESIGNING A LOW ANGLE X-RAY SCATTERING (LAXS) SYSTEM AND ITS USE IN CHARACTERISATION OF SOME BIOMEDICAL MATERIALS

by

NAGI ABDALLAH HUSSEIN

Thesis submitted in fulfilment of the requirements for
the degree of Doctor of Philosophy

May 2004

بسم الله الرحمن الرحيم

ACKNOWLEDGEMENT

First of all, plentiful thanks are due to Allah lord of the worlds.

I would like to express my sincere gratitude to my supervisor Professor A. Shukri for his assistance, guidance and support. He was always listening and caring about my being and my family. I thank him for being my supervisor and I thank him for being an older brother to me. I would like to thank my co-supervisor Professor A. A. Tajuddin for his supervision, guidance and motivations and for his kind and encouraging words since the first time we have met. My appreciation also goes to Professor C. S. Chong for his encouragement and valuable scientific guidance and for all the fruitful discussions since the early days of the project.

I am deeply indebted to my parents for their prayers and patience. May Allah bless them, amen. Special gratitude and thanks goes to my wife for taken the burden of the whole family and for standing by my side and being the source of warmth and comfort. I will never forget the joy and happiness that my sons have brought to me throughout this endeavour.

I would like to acknowledge the technical assistance and moral support provided by Mr. Azmi Omar and Mr. Habib Marikan Bawasah. The contribution and assistance of Dr. D. Bradley is greatly appreciated. The help provided by other lab. assistants and the machine workshop is also acknowledged. Finally, I would like to thank all my friends and colleagues who supported me one-way or the other and wish them all every success.

TABLE OF CONTENTS

LIST OF TABLES

LIST OF FIGURES

LIST OF SYMBOLS

μ	Attenuation coefficient
ρ	Physical density
d	Interatomic spacing
θ	Scattering angle
n	Order of diffraction
λ	Wave length
I	Intensity of X-ray beam
I_0	Initial intensity of X-ray beam
E	Energy of photon
N_A	Avogadro's number
h	Planck constant
c	Velocity of light
T	Kinetic energy
BE	Binding Energy

m_0	Rest mass of electron
e	Electron charge
$\frac{d\sigma_R}{d\Omega}$	Rayleigh differential scattering cross section
$\frac{d\sigma_{Th}}{d\Omega}$	Thomson differential scattering cross section
$\frac{d\sigma_C}{d\Omega}$	Compton differential scattering cross section
$F(q)$	Atomic form factor
f', f''	Dispersion or anomalous correction
f_{mol}	Molecular form factor
$g(q)$	Interference function
$S(q)$	Incoherent scattering function
$\vec{E}$	Electric field
$\hat{u}$	Unit vector, which represents the polarization of electric field.
E_o	Amplitude of the electric field
M	Atomic or molecular mass
Z	Atomic number

$\vec{k}$	Wave vector along direction of propagation
k	Wave number equals the magnitude wave vector
ω	Angular frequency
FWHM	Full Width at Half Maximum
FWTM	Full Width at Third Maximum
P	Photon momentum
ε_o	Permittivity of free space
x	Thickness
r	Distance
t	Time
a	Acceleration
N_o	Number of scattering centres
$\mu(q)$	Linear differential scattering coefficient
A	Cross sectional area
Ω	Solid angle
r_o	Classical electron radius or Thomson scattering length
I(q)	Final corrected diffraction pattern count
C(q)	Primary photon count
Bg(q)	Background counts

T(q)	Attenuation correction factor
SS(q)	Incident spectrum shape factor
H	Normalisation factor
σ_T	Thomson cross section
σ_{KN}	Klein-Nishina cross section
þ	Polarization factor
$\rho_e(\vec{r})$	Electron density function
$\rho(\vec{r})$	Number of electrons per unit volume.
ϕ	Phase difference
Φ	Resultant phase difference
$\vec{Q}$	Wave vector transfer
L_{TA}	Total scattering length

MEREKABENTUK SISTEM SERAKAN SINAR-X SUDUT RENDAH (LAXS) DAN PENGGUNAANNYA DALAM PENCIRIAN BEBERAPA BAHAN BIOPERUBATAN

ABSTRAK

Serakan foton sinar-X yang bertenaga diagnostik (<140 keV), pada sudut serakan kecil (<12°), daripada bahan Z rendah, secara umumnya berbentuk koheren. Ciri kekoherenan ini akan membawa kepada kesan interferens antara foton-foton yang terserak itu untuk menghasilkan corak belauan yang mempunyai kaitan dengan struktur antara-atom dan struktur antara-molekul medium serakan.

Corak-corak belauan ini menjadi tanda khusus bagi bahan yang mengalami saling tindakan berkaitan dan dengan itu boleh digunakan untuk mencirikan bahan tersebut. Corak belauan dalam kajian ini dihasilkan melalui kaedah sebaran tenaga di mana foton berbilang tenaga daripada tiub sinar-X menghentam suatu sasaran pada sudut kecil tertentu, justeru gelaran Serakan Sinar-X Sudut Rendah (LAXS). Kaedah ini juga digelar kaedah Belauan Sinar-X Sebaran Tenaga (EDXRD).

Sistem LAXS yang mematuhi prinsip-prinsip di atas telah dibina di Makmal Biofizik, Pusat Pengajian Sains Fizik, USM. Sistem tersebut terdiri daripada satu tiub sinar-X, pemasangan pengkolimat dan sasaran, pemerisaian, kelengkapan pengesanan dan kelengkapan pemerolehan data. Prestasi setiap komponen individu dalam sistem tersebut telah diuji berasingan dan ciri-ciri masing-masing direkod untuk penggunaan optimum. Sistem LAXS seterusnya diperiksa sebagai pemasangan sepadu. Penjajaran foton tuju dengan foton serakan melalui pengkolimat plumbum yang telah dibina, kearah pengesan LEGe merupakan aspek yang paling mencabar bagi kajian eksperimen tersebut.

Hasil pengoptimuman geometri bagi sistem LAXS untuk membuat keputusan tentang parameter prestasi yang terbaik boleh dirumuskan seperti berikut: tiub sinar-X harus di gunakan pada voltan gunaan 50 kV dan arus 25 mA untuk tempoh pengumpulan selama 300 saat menggunakan pengkolimat celah 2 mm dan pada sudut serakan 8° , 9° atau 10° untuk jarak tertentu yang dipilih. Kriteria yang dipilih untuk pemilihan ini adalah untuk mencapai keamatan corak belauan yang tinggi dengan puncak-puncak yang sedia terlerai dan mengandungi sebanyak mungkin perincian puncak dalam masa sesingkat mungkin.

Sistem LAXS telah digunakan dalam kajian fantom tulang yang telah difabrikasi. yang menyerupai perubahan ketumpatan tulang dalam osteoporosis. Fantom-fantom telah difabrikasi untuk mensimulasikan kehilangan tulang trabekular dan kehilangan tulang kortikal. Sistem LAXS didapati berupaya untuk membezakan antara berbagai kepekatan campuran untuk fantom-fantom tersebut dengan membandingkan corak EDXRD. Beberapa parameter kuantitatif yang mengaitkan komposisi fantom dengan ciri linear yang baik telah diwujudkan. Pengurangan dos yang diterima oleh sasaran untuk pengukuran *in vivo* masa hadapan telah dicapai melalui pengurangan masa pengumpulan tanpa kehilangan kelinearan atau kepekaan.

Contoh beberapa bahan gantian bioperubatan dan biobahan seperti air, PMMA, LLDPE, getah, tulang yang dikeringkan, tulang segar, tisu dan bahan lain telah dikaji dalam setup LAXS dan corak belauan dianalisis. Corak belaun menggambarkan struktur dan komposisi bahan. Dengan itu ianya boleh digunakan sebagai corak khusus untuk prosedur pengecaman pangkalan data masa hadapan. Bahan fantom tulang yang difabrikasi menghasilkan corak belauan yang serupa dengan corak tulang sebenar. Pekali serakan kebezaan linear bagi bahan-bahan gantian bioperubatan tersebut telah diukur.

Sebatian, campuran, logam, larutan, serbuk dan pepejal menghasilkan corak belauan tanda yang mempamerkan ketertiban struktur yang amorfus, semi amorfus atau hablur. Ini juga menunjukkan versatiliti sistem LAXS.

Sistem LAXS tersebut telah digunakan untuk mengecam bahan dengan menilaikan ruang antara-atom dan membandingkan dengan fail PDF dengan kelebihan masa pengumpulan yang pantas berbanding peleraian. Kesan ketebalan ke atas corak belauan telah dikaji untuk menentukan ketebalan optimum bagi bahan serakan. Aluminium dan kuprum digunakan untuk tujuan ini. Di samping itu kesan kepekatan dan ketumpatan larutan dikaji dengan ketumpatan jelas lebih sensitif.

ABSTRACT

Scattering of X-rays photons from low Z materials at diagnostic energies (<140 keV) and low scattering angles (<12°) is mainly coherent in nature. This coherence property will lead to interference effects between these scattered photons resulting in diffraction patterns, which are related to the interatomic and intermolecular structure of the scattering medium.

These diffraction patterns are unique signatures of the interacted materials and therefore can be used to characterise them. Diffraction patterns in this work are produced by the energy dispersive method where polyenergetic photons from an X-ray tube impinge on a target at a fixed low angles and hence the names Low Angle X-ray Scattering (LAXS). This method is also referred to as the Energy Dispersive X-Ray Diffraction (EDXRD) method.

A LAXS system that complies with the above principles has been constructed at the Biophysics Laboratory, School of Physics, USM. The system comprises an X-ray tube, collimators and target assembly, shielding, detection and data acquisition equipments. The performance of each individual component in the setup has been tested separately and its characteristics are recorded for optimal use. The LAXS system was then examined as an integrated assembly. Alignment of the incident and scattered photons through the manufactured lead collimators and into the LEGe detector was the most challenging aspect of the experimental work.

The results of geometrical optimisation of the LAXS system to decide on the best performance parameters can be summarised as follows: the X-ray tube should be working at an applied voltage of 50 kV and current of 25 mA for collection period of 300 seconds using 2 mm slit collimators and at scattering angles of 8°, 9°or 10° for certain employed distances. The criteria taken for this selection are to obtain highly intense diffraction pattern with well-resolved peaks and contain as much as possible peak details in the shortest time possible.

The LAXS system has been utilised in studying fabricated bone phantoms, which mimic the changes of bone density during osteoporosis. Phantoms were fabricated to simulate trabecular bone loss and cortical bone loss. The LAXS system was found capable to distinguish between the various mixture concentrations of theses phantoms by comparing their EDXRD patterns. Several quantitative parameters that relate to the composition of the phantoms with good linear behaviour have been established. Reduction in dose received by the target for future *in vivo* measurements was accomplished by the reduction in collection time without the loss of linearity or sensitivity.

Examples of some biomedical substitute materials and biomaterials such as water, PMMA, LLDPE, rubber, dried bone, fresh bone, tissue and others have been examined in the LAXS setup and their diffraction patterns analysed. The diffraction patterns reflected the structure and composition of the materials so that they can be used as signature patterns for future database identification procedures. Fabricated bone phantom materials gave diffraction patterns which closely resemble real bone patterns. The linear differential scattering coefficient of these biomedical substitute materials have been measured.

Compounds, mixtures, metals, solutions, liquids, powders and solids produced signature diffraction patterns that reflect their structural order being amorphous, semi amorphous or crystalline. This also serves to show the versatility of the LAXS system.

The LAXS system has been used to identify materials by evaluating their interatomic spacings and comparing them with PDF files with the advantage of fast collection time over resolution. The effect of thickness on the diffraction patterns were investigated to determine the optimal thickness of the scattering material, Aluminium and copper were used for this purpose. In addition the effect of concentration and density of solutions samples were investigated with density appearing to be more sensitive.

CHAPTER ONE

Introduction

1. 1 Introduction

Even before the discovery of X-rays by Roentgen in 1895, there was some scientific work on radiation scattering by Lord Rayleigh, and others but it was concerned with light scattering (Strutt, 1871a, 1871b). The first work on X-ray scattering by free electrons was conducted by Thomson (1906).

The subject of scattering of X-rays by crystals was addressed by Darwin (1914) among others. Bragg and Bragg got the Nobel Prize (1915) on their experimental work on X-ray diffraction. The theoretical treatment of X-ray diffraction was established soon by Ewald (1916, 1917) and then by Von Laue (1931, 1935).

X-ray diffraction technique was, and still being employed, as a method for characterisation of crystalline materials; the familiar subject of crystallography. X-ray diffraction by large molecules, which show non-crystallinity with some order on the local scale, was also tackled. Since the spacing of such molecules is quite large in the order of tens and hundreds of interatomic spacing, and by inspection of the well known Bragg diffraction equation, the restriction to the use of small scattering angle θ is clearly observed, (Guinier and Fournet, 1955). The use of a larger X-ray wavelength λ is another alternative approach to small angle scattering, but in this case, X-ray absorption

will be great as to diminish the intensity of the diffracted beam and hence burden the detector employed with such long wavelengths.

In addition to X-ray diffraction, X-ray radiation was used in imaging since the day of its discovery. The field of radiology is a well-established science. However, X-ray scattering in this field is considered a problem, (Magalhaes *et al.*, 1995) that reduces contrast and signal to noise ratio of the image and therefore, leads to low quality images. Such problematic scattering must be overcome and various procedures were used in order to minimise the effect of scattering and preserve image quality (Moore *et al.*, 1976; Stonestrom and Macovski, 1976; Rudin and Bednarek; 1980, Cack, 1981; Joseph and Spital, 1981; and Magalhaes *et al.*, 1995).

Characterisation of biomedical materials such as in the investigation of bone density using gamma-rays based on the transmission technique were done by Cameron and Sorenson (1963), Roos *et al.* (1970), West and Reed (1970), Sorenson and Mazess (1970), Bradley *et al.* (1986) and Mooney and Speller (1992) and in the characterisation of other materials by Mancini (1985) and Bradley *et al.* (1986). X-rays were also employed in this area in the work of Buchnea *et al.* (1982).

Due to the dominance of scattering cross sections over absorption cross sections for common materials and in the radiological energy range of interest 0 - 140 keV (Holt *et al.*, 1983, 1984 and Chong, 1989), scattering can be a useful tool in characterisation of materials using these energies.

Incoherent scattering is employed in the characterisation of materials in addition to transmission by several authors such as Clarke and Van Dyke (1973), Webber and Kennett (1976), and Chong (1989). The use of the ratio of the coherent to the incoherent scattered photons in the determination of bone density was the work of many authors such as Puumalainen *et al.* (1976), Kerr *et al.* (1980), Ling *et al.* (1982), Puumalainen *et*

al. (1982) and Mossop *et al.* (1987), and in the characterisation of other materials by the authors Holt *et al.* (1983), Holt *et al.* (1984), Manninen *et al.* (1984), Webster and Lillicrap (1985) Webster *et al.* (1986), Confalonieri *et al.* (1987), and Shakeshaft *et al.* (1997). Compton scattering alone was used for the purpose of imaging by Holt *et al.* (1984), and Harding and Tischler (1986) and for identification of materials by Magalhaes *et al.* (1995) or their densities by Sharaf (2001). Coherent scattering as a single process was used to measure bone density by Kerr *et al.* (1980), and Ndlovu *et al.* (1991). The Back scattering technique was employed by Mohammadi (1981), Wolf and Munro (1985), Confalonieri *et al.* (1987), Tuzi and Sato (1990), El-Kateb and Shehadah (1993), Tartari *et al.* (1994), Elyaseery and Chong (1995), Yacouti *et al.* (1997), and Morgan *et al.* (1998) for the identification of materials.

1.2 Coherent scattering

Coherent scattering has been dismissed as a process for identification of materials because of its small contribution to attenuation coefficient compared with incoherent scattering. Coherent scattered radiation does not depend on energy and its angular dependence is forward peaking, i.e. the differential scattering probability is peaked at zero and therefore indistinguishable from transmitted radiation, and in such cases it is a reducing quality process (Neitzel *et al.*, 1985).

However, calculations by Johns and Yaffe (1983) using single scatter showed that in the diagnostic energy range, the differential scattering cross section for coherent scattering did not peak at zero angle as it was previously believed but at an angle larger than zero. In fact, the differential coherent scattering cross section at zero degrees almost vanishes. The work of the above authors was concerned with water, concluded that the maximum scattering probability occurred at an angle equals to 3.8° for photon energy of 60 keV, which is attributed to intermolecular interference. Their work also

showed that coherent scattering was much greater than incoherent scattering at low angles, and it contributed significantly to the total scattering process.

Morin and Berroir (1983) also showed that the forward peaking occurs at a non-zero angle for water samples, and the ratio of a single scattered photon to transmitted one is energy dependent with a significant contribution from Rayleigh scattering to this single scatter. The experimental work carried out by Muntz *et al.* (1983) confirmed the forward peaking of differential scattering cross sections at low angles and showed that the positions of the peaks depends on the structure of the material and depends slightly on the energy. So far, only single scatter is being considered while in real systems (thick objects) multiple scattering always occurs.

The work reported by Neitzel *et al.* (1985) using Monte Carlo simulation showed the existence of incoherent multiple scattering, but the dominance is still to single scatter for these thick objects when polyenergetic radiation was used. This work also confirmed the forward peaking of coherent scattering probability at low scattering angles away from the transmitted radiation, and the broadening of the peak of interest with increasing sample thickness.

1.3 Low angle coherent scattering

An X-ray photon can interact with matter through various processes. Photoelectric effect and Compton (inelastic) scattering are the most common interactions. The most important interaction processes are dealt with in the next chapter.

There exist a type of interaction where the scattering of X-rays photons in the energy range of about 140 keV or less and at low scattering angles (< 12°) will be mainly coherent with no energy change involved in the process. This interaction is called coherent elastic scattering or historically known as Rayleigh scattering. X-ray scattering

at low angles is considered to be a coherent or elastic process due to the high probability of its cross section over incoherent (inelastic) Compton scattering cross section.

Scattering can be from a single free electron, the classical case of oscillating charge that emits radiation of the same frequency as the photons impinging on it. This is known as "Thomson scattering". Also scattering can be from bound electrons in an atom of atomic number Z and in this case, both the atomic number of the atom and momentum transfer q must be taken into account. This is usually expressed as a function F (q, Z) known as the atomic form factor. This scattering is known as "Rayleigh scattering". A detailed coverage of both interactions is given in the next chapter.

Since scattering is coherent, the scattered waves will retain the same wavelengths, as the incident waves and a definite phase relation between them will exist. Interference effects will take place and their nature will depend on the electron distribution of the target medium. Interference can be attributed to be due to three basic routes: first between scattered waves of electrons in the same atom of object molecule, secondly between scattered waves of electrons of neighbouring atoms within the same object molecule (interatomic), and thirdly between scattered waves of different molecules (intermolecular).

Furthermore, if the object material has some regular order, be it short or long order, then interference can occur between coherently scattered X-rays photons from adjacent atomic planes, at some small angle θ. Diffraction will then occur and is governed by Bragg law which is given by

$$n\lambda = 2d \sin\frac{\theta}{2} \qquad (1.1)$$

where n is the order of the diffraction, λ is the wavelength of incident X-ray photon, θ is the scattering angle, and d is interatomic spacing of the material. This equation can be expressed in terms of energy as follows

$$\frac{1}{E} = \frac{2d}{n\,h\,c} \sin\frac{\theta}{2} \qquad (1.2)$$

where E is the energy of the incident X-ray photon, h is Planck's constant and c is the velocity of light.

The diffraction pattern obtained is composed of the energy spectrum of the incident X-ray source with the diffraction effects superimposed upon it. This diffraction pattern will be a characteristic of that object material.

Inspection of Equation 1.1 and Equation 1.2 shows clearly two distinctive methods of obtaining diffraction patterns. Keeping the incident wavelength λ of X-ray photon fixed by the use of monoenergetic photons and sweeping the various angles θ will give a diffraction pattern. This technique is known as the angular dispersive method and it is common in the field of crystallography. The alternative method is to keep θ fixed at a given angle and vary the wavelength of the X-ray source and this usually done by employing a polyenergetic X-ray source where the various wavelengths exist together, via the use of an X-ray tube. This technique is known as the energy dispersive method and will be used in this work.

Therefore, the phenomenon of Low Angle X-ray Scattering (LAXS) or Energy Dispersive X-Ray Diffraction (EDXRD) can be exploited to characterise materials of low atomic number Z that have some order in their structure. This is done by obtaining a diffraction pattern, a "signature" pattern specific of the material under investigation since it depends on its molecular structure. X-ray diffraction effects although more pronounced in crystalline substances than amorphous substances, do not only result

from separations of atomic planes within the crystal, but occur due to any appropriate separation of electrons (Royle and Speller, 1995).

Giessen and Gordan (1968) earlier investigated this phenomenon of Low Angle X-ray Scattering (LAXS), by irradiating powdered samples with polychromatic radiation from an X-ray tube. The scattered X-ray spectra at low angle (~ 10°) were collected using a semiconductor detector and the lattice spacings of the samples were then deducted. Energy Dispersive X-Ray Diffraction (EDXRD), employing low angle X-ray scattering from synchrotron radiation was used by Bordas *et al.* (1976) to study biological samples. This LAXS technique is used to investigate the bulk structure of materials, particularly with low Z materials, that have some local order.

There is another technique, which is reported extensively in the literature by many authors such as Guinier and Fournet (1955), Kaelble (1967), and Glatter and Kratky (1982), namely Small Angle X-ray Scattering (SAXS) which should not be confused with LAXS. Though they are similar in certain general aspects, SAXS is used to investigate particle size and scattering is due to the particle and not to the internal structure it possesses and therefore Bragg diffraction cannot be employed. In addition, SAXS experiments employ angular dispersive method in its analysis.

1.4 Applications of LAXS

Since in LAXS the scattered X-ray photons have interacted with the target medium then they carry with them information relating to that medium which cannot be said about transmission based techniques. The phenomenon of low angle X-ray scattering (LAXS) or energy dispersive X-ray diffraction (EDXRD) has some solid theoretical and experimental support to be exploited in the field of material identification. It is not surprising to see that the first application of low angle X-ray scattering was a medical

application, and in the field of radiology in particular, since most of the previously mentioned works were in the field of radiology too. Harding *et al.* (1985, 1987) experimented on a computed tomography imaging system based on low angle X-ray scattering.

The applications of low angle X-ray scattering may be categorised mainly into two fields: the medical and industrial. The development of the LAXS technique in these fields will be discussed in some detail. The medical field includes computed tomography, bone mineral density determination, characterisation of biomedical materials and imaging, and characterisation of related materials. The industrial field includes the studies of food contaminants, spices, explosives, and other materials of interest.

1.4.1 Computed tomography

Coherent X-ray scattering in computed tomography was covered by several authors such as Harding *et al.* (1985, 1987, 1990), Westmore *et al.* (1995, 1997), Barroso *et al.* (1998), and Hall *et al.* (1998).

1.4.2 Bone analysis and mineral density determination

As discussed previously, almost all the work on the measurement of bone mineral density was done using gamma-rays as the source of radiation. However, in the work done by Webster and Lillicrap (1985) a heavily filtered X-ray beam was used to determine bone mineral density. The LAXS technique for bone analysis was utilised by Royle and Speller (1991, 1995), Farquharson *et al.* (1997), Farquharson and Speller (1998) and Allday and Farquharson (2001).

1.4.3 Characterisation of biomedical materials and diagnostic radiology

There are many documented research in these areas using coherent X-ray scattering such as Bordas *et al.* (1976) (rat tail tendon), Johns and Yaffe (1983) (water), Morin and Berroir (1983) (water), Muntz *et al.* (1983) (perspex), Neitzel *et al.* (1985), Kosanetzky *et al.* (1987) (muscle), Evans *et al.* (1991), Speller and Horrocks (1991), Royle and Speller (1995) (bone), Chapman *et al.* (1997), Tartari *et al.* (1997), Byng *et al.* (1998) (breast tissue), Peplow and Verghese (1998), Bradley *et al.* (1999b), Elshemey, *et al.* (1999), Kidane *et al.* (1999) (breast tissue), Royle *et al.* (1999), Barroso *et al.* (2000), Desouky *et al.* (2001) (blood), Elshemey *et al.* (2001) and Poletti *et al.* (2002). Details of some of the above authors can be seen on chapter three

1.4.4 Characterisation of other materials

The materials covered in this section are medical substitute material or other non-medical materials such as Pt, Au, SiC, plastics, stainless steel, oil etc. Authors who reported in this area are: Giessen and Gordan (1968), Kosanetzky *et al.* (1987), Zhu *et al.* (1994), Iwanczyk *et al.* (1995), Westmore *et al.* (1996), Peplow and Verghese (1998), Bomsdorf (1999), Luggar *et al.* (1999) and Bomsdorf and Kosanetzky (2000). See chapter three for more details.

1.4.5 Food industry

Measurements of contaminants in food were studied by authors such as Martens *et al.* (1993) and Bull *et al.* (1997). Spices were studied using the LAXS technique by Desouky *et al.* (2002).

1.4.6 Detection of explosives

There are several methods, which can be employed in the detection of explosives. Summarised accounts of such methods and the vital role they play in airport security

have been reported by Stix (1992), George (1996), Nelms *et al.* (1999) and Speller (2001). The low angle X-ray scattering technique was employed in the detection of explosives by several authors such as Luggar *et al.* (1997), Luggar (1998), Luggar *et al.* (1998), Malden and Speller (2000) and Hastings *et al.* (2001). A good review on the above material can be found in the paper written by Luggar and Gilboy (1999).

1.4.7 Others

Theoretical treatment and other experimental aspects of the subject are well covered by the following authors Kissel *et al.* (1980), Roy (1980), Pratt (1983), Kane *et al.* (1986), Bradley *et al.* (1989), Saha (1995), Luggar *et al.* (1996), Farquharson *et al.* (1997), Rao *et al.* (1997), Luggar *et al.* (1998), Bradley *et al.* (1999a), Bradley *et al.* (1999b), Roy *et al.* (1999), Sidhu *et al.* (1999), Tartari (1999), Carney (2000), Tartari *et al.* (2000) Carney and Pratt (2001), and Tartari *et al.* (2002).

1.5 Scope of work

The scope of this work can be summarised in the following points:

- Characterisation of materials using a LAXS system comes in as a natural research project in the research scheme of the biophysics group at the school of physics, USM.
- Set up of the system is considered the first phase to be undertaken in the project. This phase involves the individual testing of the equipments in the LAXS set up; the X-ray machine, the X-ray photon detector and the supporting electronic gadgets.
- The initial phase also includes the selecting and fabrication of collimators, collimators stands, movable arm for selecting angles and shielding.

- Experimental works were carried out on all the above aspects to determine their features and working conditions and hence evaluate each component individually and as part of the designed scattering scheme.
- The second phase of the project involves experimental work on the previously examined LAXS system setup using a standard crystalline material. Calcium carbonate powder was employed for this purpose.
- Parameters that affect the performance of the LAXS system were studied extensively and evaluated in order to optimise the best working condition of the system. The main parameters studied were: current, applied voltage, type and size of collimation system and time of exposure.
- The third phase of the projects deals with some applications of the LAXS system.

1.6 Objectives

The objectives of this work are to design an LAXS system, optimise it and utilise it in several applications, which were categorised as follows:

(i) Scattering from pure solids, compounds and mixtures

(ii) Scattering from powders and liquids

(iii) Scattering from some biomedical materials

(iv) Scattering from simulated bone phantoms to study changes in bone matrix densities and cortical bone thicknesses.

(v) Study of some physical factors that effect sensitivity of LAXS.

(vi) Evaluation of interatomic spacings of certain substances.

(vii) Determination of linear differential scattering coefficient of some biomedical substitute materials.

CHAPTER TWO

Theoretical Background

2.1 Interaction of X-rays with matter

An X-ray photon can interact with the medium it is traversing by many processes. In general, X-ray photons can be either absorbed or scattered. A collimated beam of X-ray photons has an exponential absorption nature, since each X-ray photon is absorbed or scattered in one single event which means that any photon, in the incident beam, passes the material had no interaction what so ever. The absorption law can be written as follows

$$I = I_o \, e^{-\mu x} \tag{2.1}$$

where, I_0 is the initial intensity, I intensity after passing a medium of thickness x, and μ is the linear attenuation coefficient. The possible processes of X-ray photon interactions can be deducted from the classification done by Fano (1953), which depends on both the type and effect of the interactions as seen in Table 2.1.

Table 2.1: Type and effect of possible interaction processes

Type of interaction	Effect of interaction
1. interaction with atomic electrons	**a.** complete absorption
2. interaction with nucleons	**b.** elastic (coherent) scattering
3. interaction with electric field surrounding nuclei or electrons	**c.** inelastic (incoherent) scattering
4. interaction with meson field surrounding nucleons	

There are twelve combinations between the two columns representing the possible interaction processes that can be obtained. Some processes dominate over others depending on the energy range. The processes of interest can be listed as follows:

(i) Photoelectric effect (1a)

(ii) Compton scattering (1c)

(iii) Pair production (3a)

(iv) Rayleigh Scattering (1b)

(v) Nuclear Thomson scattering (2b)

(vi) Delbruck scattering (3b)

(vii) Nuclear resonance scattering (2c)

(viii) Photo disintegration of nuclei (2a)

(ix) Meson production (4a)

In the energy range from a few keV up to a few MeV, the most common processes are the first three processes listed above in addition to the Rayleigh scattering process. A brief description of those processes, which are considered to be useful is given below.

2.1.1 Photoelectric effect

This process occurs in the energy range 1 – 100 keV, and it involves the removal of bound electrons from the atoms upon the absorption of all the incident photon energy. The energy of the photon, E should be equal to or larger than the electron binding energy, BE. For the latter case, an electron will be ejected with kinetic energy, T given by

$$T = E - BE \tag{2.2}$$

2.1.2 Compton scattering

This process dominates at intermediate energy, and it deals with the scattering of X-ray photons by atomic electrons that are assumed free, therefore, it occurs at energies greater than the binding energy of the electrons. For an X-ray photon with energy, E, it will scatter, upon striking a target electron, through angle, θ, made relative to the original direction and with energy E', given by

$$E' = \frac{E}{1 + \frac{E}{m_0 c^2}(1 - \cos\theta)} \tag{2.3a}$$

where, m_0 represents the mass of electron and c the velocity of light.

The differential total Compton cross section is given by

$$\frac{d\sigma_C}{d\Omega} = \frac{d\sigma_{KN}}{d\Omega} S(q) \tag{2.3b}$$

where the first term refers to the Klein-Nishina function and the second term is the incoherent atomic scatter function.

2.1.3 Pair production

When the photon energy exceeds 1.02 MeV ($m_0 c^2$), annihilation of the photon occurs with the appearance of electron - positron pair in its place. The electron - positron pair has a total kinetic energy equal to the energy of the vanished photon.

$$E - 2m_o c^2 = T_{e^-} + T_{e^+} \tag{2.4a}$$

where T_{e^-} and T_{e^+} are the kinetic energies of the electron and positron respectively. This process will only take place greatly in the field of the nucleus and takes over as the dominant process as the photon energy increases.

2.1.4 Rayleigh scattering

The Compton scattering process is an inelastic (incoherent) interaction where the scattered photon suffers deviation from its original direction, and carries a lower energy than the incident one. The Rayleigh scattering process, on the other hand, is an elastic (coherent) interaction where the incident photon does not lose any energy, but suffers deviation of small angles from its original direction so that no atomic excitation or ionization occurs to the atom. The Rayleigh scattering cross section, (White, 1950), of great importance at small photon energies, but it diminishes at higher energies due to the increased dominance of the inelastic process. The differential elastic cross section is given by

$$\frac{d\sigma_R}{d\Omega} = \frac{d\sigma_{Th}}{d\Omega} F^2(q) \tag{2.4b}$$

where the first term refers to Thomson cross section and the second term is the form factor scatter function.

Elastic scatter is predominant at small angles and in the diagnostic energy range or low momentum transfers that is single coherent scatter is much more intense than single

Compton scatter. Within this region, single inelastic scatter is suppressed due to electron binding effects. Nevertheless, this is in conflict with the fact that the total inelastic cross-section is greater than the total elastic scatter cross-section (about 10 %). For example, the partial interaction cross-sections for oxygen over the diagnostic energy region (0-100 keV) shows photon attenuation is dominated by photoelectric absorption and incoherent (Compton) scatter and at no point is elastic scatter the major influence. This conflict is resolved by observing the differential cross-sections for scatter in the momentum range below 0.5 $Å^{-1}$ (corresponding to 10° at 70 keV) where coherent scatter is the dominant mechanism for photon scattering. By comparing both the coherent form factor function and the incoherent scattering function below the momentum transfer value stated above, it can be said that the coherent scatter is confined to a narrow forward scattering peak and the Compton scatter vanishes as the momentum transfer approaches zero due the incoherent scattering function. A detailed outline of this process will be given later.

2.1.5 Nuclear Thomson scattering

This is another type of elastic scattering which, combines coherently with Rayleigh scattering. It is detected at high energies, and attributed to the scattering from the nucleus, which is considered to be a point charge. This interaction has small contributions due to the large mass of the nucleus, (Davey, 1953; Strickler, 1953; Wilson, 1953).

2.1.6 Delbruck scattering

Delbruck scattering is also an elastic (coherent) scattering process, and is due to the formation of virtual electron-positron pair in the field of the nucleus followed by annihilation in the same field. It takes place at energies above 1 MeV.

2.1.7 Nuclear resonance scattering

This process is an elastic one and occurs at energies above 1 MeV. It involves the excitation of the nuclear levels by the impinging photon followed by emission of this excitation energy, and it also involves nuclear resonance giant dipole transitions.

2.1.8 Photo disintegration of nuclei

This process is referred to as the nuclear photoeffect, it takes place when the energy of the photon is larger than the nucleon separation energy and it is restricted to energies above 8 MeV. This absorption process has very small cross sections.

2.1.9 Meson production

Meson production is an absorbing process, which requires high photon energy in the range of about 150 MeV. The cross section associated with this process is negligible.

2.2 Principles of X-ray scattering

2.2.1 Introduction

X-rays are electromagnetic waves that consist of electrical fields, $\vec{E}$ and magnetic fields, $\vec{B}$ perpendicular to each other and to the direction of propagation. Electromagnetic waves can be represented by a plane wave expressed in terms of the electric field vector $\vec{E}$. For linearly polarized electromagnetic waves, it can be written in general in the form

$$\vec{E}(\vec{r},t) = \hat{u}E_o e^{i(\vec{k}.\vec{r}-\omega t)} \qquad (2.5)$$

where, $\vec{k}$ is wave vector along the direction of propagation and its magnitude $k = \frac{2\pi}{\lambda}$ is called the wave number, λ is the wavelength. E_0, is the amplitude of the

electric field, ω is angular frequency, and $\hat{u}$, is a unit vector, which represents the polarization of electric field. If the direction of propagation is assumed to be along the z– axis then Equation (2.5) can be simplified by taking its real part, to

$$\vec{E}(z,t) = \hat{u}E_0 \sin\ (kz - \omega t) \tag{2.6}$$

The above description is a classical one. The quantum mechanical conception of an electromagnetic wave is one consisting of photons each carrying definite amounts of energy called "quantum". The energy of the photon E is given by

$$E = \hbar\omega \tag{2.7}$$

The photon also has a momentum P associated with it given by

$$P = \hbar k \tag{2.8}$$

The intensity I of an X-ray beam equals the number of photons per second that transverses a given area. Classically, the intensity of X-ray beam is proportional to the square of the electric field.

$$I \propto \left|\vec{E}^{\,2}\right| \tag{2.9}$$

2.2.2 Scattering of X-rays by single electron "Thomson scattering"

When an X-ray photon of low energy ($\hbar\omega << mc^2$) strikes a single electron, the electric field of the incident electromagnetic wave will exert a force on it. According to the classical theory of radiation, the electron will accelerate and therefore will emit an electromagnetic radiation of the same wavelength as the incident one that represents the scattered wave. This is a description of an elastic process. Note that in this classical view momentum transfer is ignored. In fact, some momentum is bound to be transferred to the electron since any photon has momentum given by Equation (2.8).

If the electron is bound to an atom, the incident photon's momentum will be transferred not to the electron concerned but to the whole atom. In this case, the energy loss will be given by

$$E_{loss} = \frac{P^2}{2M} \tag{2.10}$$

where M is the atomic mass and not the electronic mass m_o.

Since $M >> m_o$, then the energy of the scattered photon is almost unchanged from the incident one and the process remains an elastic process. An elastic process, therefore, can involve momentum transfer to some extent.

Consider a free electron that is struck by an electromagnetic plane polarised radiation with its electric vector in the y-z plane given by

$$\vec{E}_{in} = \vec{E}_{oy} e^{-i\omega t} \tag{2.11}$$

The electronic charge will be accelerated back and forth along the y-axis in very small amplitudes. The field, at some observation point P, which is at a distance r from the electron and makes an angle θ with respect to the direction of travel, must be calculated. The observer can be located either in the y-z plane (i.e. in a plane of polarisation of the incident wave) at P1 or in the x-z plane (i.e. in plane perpendicular to the plane of polarisation) at P2, as in Fig. 2.1.

The radiated field at point P is given by

$$\vec{E}_{rad}(r,t) = -\frac{-e\,a(t-\frac{r}{c})}{4\pi\varepsilon_o c^2 r} \tag{2.12}$$

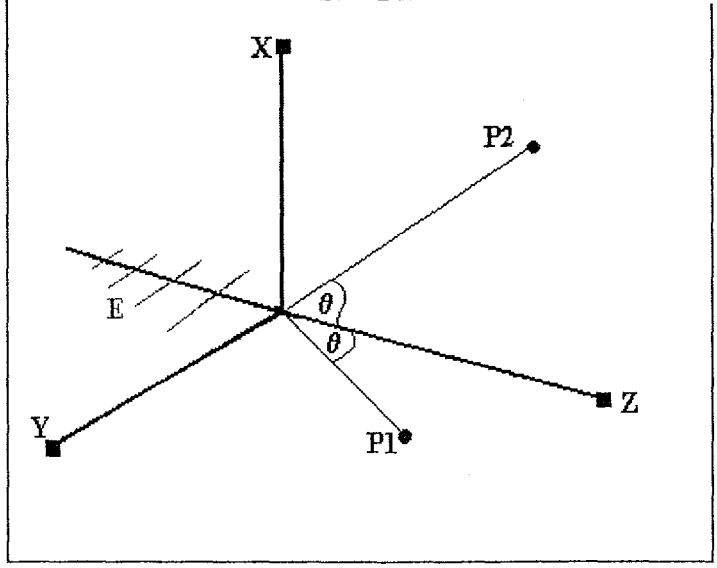

Fig. 2.1 Coordinate axes and observer points for EM wave of electric field E.

where, $a\,(t-\frac{r}{c})$ is the acceleration at time $(t-\frac{r}{c})$, which is called the retarded acceleration, and should be the component of acceleration perpendicular to the line of sight (Feynman *et al.*, 1965). In this case it equals to $a(t-\frac{r}{c})\cos\theta$. Therefore, Equation (2.12) becomes

$$\vec{E}_{rad}(r,t) = \frac{-e\,a\,(t-\frac{r}{c})\cos\theta}{4\pi\varepsilon_o c^2\, r} \tag{2.13}$$

It can be noted that if $\theta = \frac{\pi}{2}$ then a = 0 and hence no acceleration is observed, and if $\theta = 0$, the full acceleration is observed at that position. Therefore, if the observer is at position P2, the acceleration at any point in that plane is perpendicular to the line of sight and the radiated field will be give by Equation (2.12). The acceleration is related to the electric field by the following relation

$$a = \frac{-e}{m_e}\vec{E}_{in} \tag{2.14}$$

Using Equation (2.11), $k = \frac{\omega}{c}$ and then rearranging to obtain

$$a(t - \frac{r}{c}) = \frac{-e}{m_e}\vec{E}_{in}\, e^{ikr} \tag{2.15}$$

Therefore, Equation (2.12) becomes

$$\vec{E}_{rad}(r,t) = -\frac{e^2}{4\pi\varepsilon_o m_e c^2}\frac{e^{ikr}}{r}\vec{E}_{in} \tag{2.16}$$

And Equation (2.13) becomes

$$\vec{E}_{rad}(r,t) = -\frac{e^2}{4\pi\varepsilon_o m_e c^2}\frac{e^{ikr}}{r}\vec{E}_{in}\cos\theta \tag{2.17}$$

The first term is defined as r_o the classical electron radius or sometimes it is known as *Thomson scattering length* $r_o = \frac{e^2}{4\pi\varepsilon_o m_e c^2} = 2.82 \times 10^{-15}\, m$, and the second term $\frac{e^{ikr}}{r}$, represents a spherical wave. Equation (2.16) and Equation (2.17) can be written as the ratio between the radiated or scattered electric field and the incident electric field.

$$\frac{\vec{E}_{rad}}{\vec{E}_{in}} = -r_o\frac{e^{ikr}}{r} \tag{2.18}$$

$$\frac{\vec{E}_{rad}}{\vec{E}_{in}} = -r_o\frac{e^{ikr}}{r}\cos\theta \tag{2.19}$$

Note that in all the above equations the minus sign is there to indicate that the scattered field is 180° out of phase with the incident field and therefore, the scattering process involves a phase shift equal to π.

The differential scattering cross section, $\frac{d\sigma}{d\Omega}$, is defined as:

$$\frac{d\sigma}{d\Omega} = \frac{number\ of\ X-rays\ scattered\ per\ second\ in\ solid\ angle\ \Delta\Omega}{incident\ flux \times \Delta\Omega} \tag{2.20}$$

Let us define scattering intensity, I_s as the number of photons per second recorded by the detector, and incident intensity, I_{in} as the number of incident photons per second.

The incident flux is given by the relation, $\frac{I_{in}}{A_{in}}$ which can be written as

$$\frac{I_s}{I_{in}} = \frac{\left|\vec{E}_{rad}\right|^2 r^2 \Delta\Omega}{\left|\vec{E}_{in}\right|^2 A_{in}} \tag{2.21}$$

where, $\Delta\Omega$ is the solid angle subtended by the detector, $r^2\Delta\Omega$ is the cross sectional area of the scattered beam and A_{in} is the cross sectional area of the incident beam. Hence, Equation (2.20) becomes

$$\frac{d\sigma}{d\Omega} = \frac{\left|\vec{E}_{rad}\right|^2}{\left|\vec{E}_{in}\right|^2} r^2 \tag{2.22}$$

Substitute into Equation (2.19), one obtains

$$\frac{d\sigma}{d\Omega} = r_o^2(\cos^2\theta) \tag{2.23}$$

This is the differential coherent scattering cross section for an X-ray beam with polarisation in the scattering plane. Substitute into Equation (2.18), one obtains

$$\frac{d\sigma}{d\Omega} = r_o^2 \qquad (2.24)$$

This is the differential coherent scattering cross section for an X-ray beam with polarisation perpendicular to the scattering plane.

For unpolarized X-rays, the incident electric field is equally probable in the x-y plane and its average value is given by $\langle \vec{E}_{in}^{\,2} \rangle = \langle \vec{E}_{x}^{\,2} \rangle + \langle \vec{E}_{y}^{\,2} \rangle$ but the last two components will be equal when averaged over many photons and will be equal to $\frac{\langle \vec{E}_{in}^{\,2} \rangle}{2}$. Therefore,

$$\left| \vec{E}_{rad} \right|^2 = \frac{r_0^2}{r^2} \frac{\langle \vec{E}_{in}^{\,2} \rangle}{2} (1 + \cos^2 \theta) \qquad (2.25)$$

We can substitute, into Equation (2.22), to obtain

$$\frac{d\sigma_{Th}}{d\Omega} = \frac{1}{2} r_o^2 (1 + \cos^2 \theta) \qquad (2.26)$$

This is the differential coherent scattering cross section for an unpolarized X-ray beam, known as the Thomson formula. The total coherent scattering cross section, σ_T, can be obtained by integrating over all possible scattering angles, θ.

$$\sigma_T = \frac{8\pi}{3} r_0^2 \qquad (2.27)$$

$$\sigma_T = 0.665 \times 10^{-28}\ m^2 = 0.665\ barn.$$

Concluding remarks

- The total or differential classical scattering cross section by free electrons is constant and independent of energy.
- The polarization factor, þ, which depends on the X-ray source has values of þ = 1, for electric field perpendicular to the scattering plane.

$\text{þ} = \cos^2\theta$, for electric field in the scattering plane.

$\text{þ} = \frac{1}{2}(1+\cos^2\theta)$, for unpolarized source.

- The differential scattering cross section, in units of r_o^2, $\frac{d\sigma/d\Omega}{r_0^2}$ fluctuates in magnitude between 1 for scattering angle 0 and π and $\frac{1}{2}$ when scattering angle equals $\frac{\pi}{2}$.

- The Klein- Nishina formula is given by

$$\sigma_{KN} = r_0^2 \frac{8\pi}{3}(1 - \frac{2\hbar\omega}{m_o c^2} + \cdots) \qquad \text{for } \hbar\omega << m_o c^2$$

$$\sigma_{KN} = r_0^2 \frac{\pi m_o c^2}{\hbar\omega}[\ln(\frac{2\hbar\omega}{m_o c^2}) + \frac{1}{2}] \qquad \text{for } \hbar\omega >> m_o c^2$$

At low photon energies, much less than the electron's rest mass energy, the Klein-Nishina cross section, σ_{KN} approaches Thomson scattering cross section, σ_T. At high photon energies, quantum mechanical effects appear and the cross section departs from the Thomson scattering cross section.

2.2.3 Scattering of X-rays by an atom "Rayleigh scattering"

For an atom with Z with electrons, scattering is considered to be from the cloud of electrons surrounding the nucleus, which acts as the origin of coordinates (Cowley, 1975). Each electron has a distribution function or electron density function, $\rho_e(\vec{r})$, which gives the probability that an electron is confined to a volume element at position $\vec{r}$. This process is known as Rayleigh scattering.